

Multifractal Analysis of Various PDF in Turbulence based on Generalized Statistics: A Way to Tangles in Superfluid He

Toshihico Arimitsu^{*†} and Naoko Arimitsu^{**}

^{*}*Institute of Physics, University of Tsukuba, Ibaraki 305-8571, Japan*

[†]*E-mail: arimitsu@cm.ph.tsukuba.ac.jp*

^{**}*Graduate School of EIS, Yokohama Nat'l. University, Yokohama 240-8501, Japan*

Abstract. By means of the multifractal analysis (MFA), the expressions of the probability density functions (PDFs) are unified in a compact analytical formula which is valid for various quantities in turbulence. It is shown that the formula can explain precisely the experimentally observed PDFs both on log and linear scales. The PDF consists of two parts, i.e., the *tail* part and the *center* part. The structure of the tail part of the PDFs, determined mostly by the intermittency exponent, represents the intermittent large deviations that is a manifestation of the multifractal distribution of singularities in physical space due to the scale invariance of the Navier-Stokes equation for large Reynolds number. On the other hand, the structure of the center part represents small deviations violating the scale invariance due to thermal fluctuations and/or observation error.

INTRODUCTION

In this paper, we derive the unified formula for various probability density functions (PDFs) in fully developed turbulence by means of the *multifractal analysis* (MFA) [1, 2, 3, 4, 5, 6, 7, 8, 9, 10, 11, 12], and analyze the PDFs observed in two experiments, i.e., the PDFs of velocity fluctuations, of velocity derivatives and of fluid particle accelerations at $R_\lambda = 380$ that was extracted by Gotoh et al. from the DNS of the size 1024^3 [13], and the PDF of fluid particle accelerations at $R_\lambda = 690$ obtained in the Lagrangian measurement of particle accelerations that was realized by Bodenschatz and co-workers [14, 15, 16] by raising dramatically the spatial and temporal measurement resolutions with the help of the silicon strip detectors. The MFA of turbulence is a unified self-consistent approach for the systems with large deviations, which has been constructed based on the Tsallis-type distribution function [17, 18] that provides an extremum of the *extensive* Rény [19] or the *non-extensive* Tsallis entropy [17, 18, 20] under appropriate constraints. The analysis rests on the scale invariance of the Navier-Stokes equation for high Reynolds number, and on the assumptions that the singularities due to the invariance distribute themselves multifractally in physical space. The MFA is a generalization of the log-normal model [21, 22, 23]. It has been shown [5] that the MFA derives the log-normal model when one starts with the Boltzmann-Gibbs entropy.

For high Reynolds number $Re \gg 1$, or for the situation where effects of the kinematic viscosity ν can be neglected compared with those of the turbulent viscosity, the Navier-Stokes equation, $\partial \mathbf{u} / \partial t + (\mathbf{u} \cdot \nabla) \mathbf{u} = -\nabla(p/\rho) + \nu \nabla^2 \mathbf{u}$, of an incompressible fluid is

invariant under the scale transformation [24, 25, 26] $\mathbf{r} \rightarrow \lambda \mathbf{r}$, $\mathbf{u} \rightarrow \lambda^{\alpha/3} \mathbf{u}$, $t \rightarrow \lambda^{1-\alpha/3} t$ and $(p/\rho) \rightarrow \lambda^{2\alpha/3} (p/\rho)$ where the exponent α is an arbitrary real quantity. The quantities ρ and p represent, respectively, mass density and pressure. The Reynolds number Re of the system is given by $\text{Re} = \delta u_{\text{in}} \ell_{\text{in}} / \nu = (\ell_{\text{in}} / \eta)^{4/3}$ with the Kolmogorov scale $\eta = (\nu^3 / \epsilon)^{1/4}$ [27] where ϵ is the energy input rate at the input scale ℓ_{in} . Here, we introduced $\delta u_{\text{in}} = |u(\bullet + \ell_{\text{in}}) - u(\bullet)|$ with the definition of the velocity fluctuation (difference) $\delta u_n = |u(\bullet + \ell_n) - u(\bullet)|$ where u is a component of velocity field \mathbf{u} , and ℓ_n is a distance between two points. The *pressure* (divided by the mass density) difference $\delta p_n = |p/\rho(\bullet + \ell_n) - p/\rho(\bullet)|$ between two points separated by the distance ℓ_n is another important observable quantity. We are measuring distance by the discrete units $\ell_n = \delta_n \ell_0$ with $\delta_n = 2^{-n}$ ($n = 0, 1, 2, \dots$). The non-negative integer n can be interpreted as the *multifractal depth*. However, we will treat it as positive real number in the analysis of experiments. The multifractal depth n is related to the number of steps within the energy cascade model.¹ At each step of the cascade, say at the n th step, eddies break up into two pieces producing an energy cascade with the energy-transfer rate ϵ_n that represents the rate of transfer of energy per unit mass from eddies of size ℓ_n to those of size ℓ_{n+1} .

SINGULARITIES AND SCALING EXPONENTS

Let us consider the quantity $\delta x_n = |x(\bullet + \ell_n) - x(\bullet)|$ having the scaling property $|x_n| \equiv |\delta x_n / \delta x_0| = \delta_n^{\phi\alpha/3}$. Its spatial derivative is defined by $|x'| = \lim_{\ell_n \rightarrow 0} \delta x_n / \ell_n \propto \lim_{n \rightarrow \infty} \ell_n^{\phi\alpha/3 - 1}$ which becomes singular for $\alpha < 3/\phi$. The values of exponent α specify the degree of singularity. We see that the scale invariance provides us with $\delta u_n / \delta u_0 = \delta_n^{\alpha/3}$ and $\delta p_n / \delta p_0 = (\ell_n / \ell_0)^{2\alpha/3}$ giving, respectively, $\phi = 1$ for the velocity fluctuation and $\phi = 2$ for the pressure fluctuation. The velocity derivative and the fluid particle acceleration may be estimated, respectively, by $|u'| = \lim_{n \rightarrow \infty} u'_n$ and by $|\mathbf{a}| = \lim_{n \rightarrow \infty} a_n$ where we introduced the n th velocity derivative $u'_n = \delta u_n / \ell_n$ and the n th fluid particle acceleration $a_n = \delta p_n / \ell_n$ corresponding to the characteristic length ℓ_n . Note that the acceleration \mathbf{a} of a fluid particle is given by the substantive time derivative of the velocity: $\mathbf{a} = \partial \mathbf{u} / \partial t + (\mathbf{u} \cdot \nabla) \mathbf{u}$. We see that the velocity derivative and the fluid particle acceleration become singular for $\alpha < 3$ and $\alpha < 1.5$, respectively, i.e., $|u'| \propto \lim_{\ell_n \rightarrow 0} \ell_n^{(\alpha/3) - 1} \rightarrow \infty$ and $|\mathbf{a}| \propto \lim_{\ell_n \rightarrow 0} \ell_n^{(2\alpha/3) - 1} \rightarrow \infty$. We also see that the energy dissipation rate becomes singular in the limit $n \rightarrow \infty$ for $\alpha < 1$, i.e., $\lim_{n \rightarrow \infty} \epsilon_n / \epsilon_0 = \lim_{n \rightarrow \infty} (\ell_n / \ell_0)^{\alpha - 1} \rightarrow \infty$ giving $\phi = 3$.

The MFA rests on the multifractal distribution of singularities that is a manifestation of the scale invariance of the Navier-Stokes equation for large Re as mentioned above. The probability $P^{(n)}(\alpha) d\alpha$ to find, at a point in physical space, a singularity labeled by an exponent in the range $\alpha \sim \alpha + d\alpha$ is given by [2, 3, 4, 5]

¹ The definition of the number of steps \bar{n} within the energy cascade model is given by $\bar{n} = -\log_2(r/\ell_{\text{in}})$ for the eddies whose diameter is equal to r . By putting $r = \ell_n$, this gives us the relation between \bar{n} and n in the form

$$\bar{n} = n - \log_2(\ell_0/\ell_{\text{in}}). \quad (1)$$

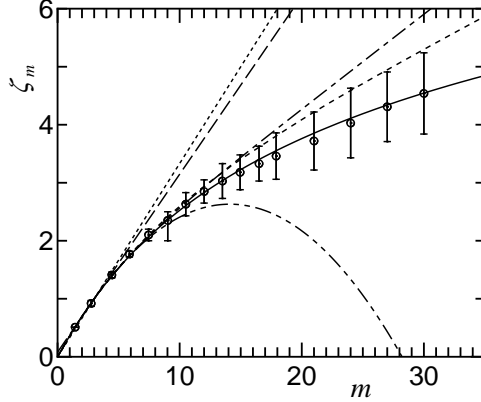


FIGURE 1. Comparison of the present scaling exponents ζ_m for $\mu = 0.238$ (solid curve) with the experimental results plotted by circles at $R_\lambda = 110$ ($\text{Re} = 32000$) [30], and with other theories with the same value of μ . K41 is given by the dotted line, β -model by the dashed line, p-model by the dotted dashed line, log-Poisson model by the short dashed curve, and log-normal by the two dotted dashed curve.

$P^{(n)}(\alpha) = [1 - (\alpha - \alpha_0)^2 / (\Delta\alpha)^2]^{n/(1-q)} / Z_\alpha^{(n)}$ with an appropriate partition function $Z_\alpha^{(n)}$ and $(\Delta\alpha)^2 = 2X / [(1-q) \ln 2]$. This is consistent with the relation [26, 5] $P^{(n)}(\alpha) \propto \delta_n^{1-f(\alpha)}$ that reveals how densely each singularity, labeled by α , fills physical space. In the present model, the multifractal spectrum $f(\alpha)$ is given by [2, 3, 4, 5] $f(\alpha) = 1 + (1-q)^{-1} \log_2 [1 - (\alpha - \alpha_0)^2 / (\Delta\alpha)^2]$. The range of α is $\alpha_{\min} \leq \alpha \leq \alpha_{\max}$ with $\alpha_{\min} = \alpha_0 - \Delta\alpha$, $\alpha_{\max} = \alpha_0 + \Delta\alpha$. The distribution function $P^{(n)}(\alpha)$ is determined by taking an extremum of generalized entropies, i.e., the *extensive* Rényi entropy or the *non-extensive* Tsallis entropy, under the condition that the information one has for the system is only the value of the intermittency exponent. In spite of the different characteristics of the entropies, the distribution functions $P^{(n)}(\alpha)$ giving their extremum have the common structure.²

The dependence of the parameters α_0 , X and q on the intermittency exponent μ is determined, self-consistently, with the help of the three independent equations, i.e., the energy conservation: $\langle \epsilon_n \rangle = \epsilon$, the definition of the intermittency exponent μ : $\langle \epsilon_n^2 \rangle = \epsilon^2 \delta_n^{-\mu}$, and the scaling relation³: $1/(1-q) = 1/\alpha_- - 1/\alpha_+$ with α_\pm satisfying $f(\alpha_\pm) = 0$. The average $\langle \dots \rangle$ is taken with $P^{(n)}(\alpha)$.

The scaling exponents ζ_m of the m th order velocity fluctuations, defined by $\langle |u_n|^m \rangle = \langle \delta_n^{m\alpha/3} \rangle \propto \delta_n^{\zeta_m}$, are given in the analytical form [2, 3, 4, 5]

$$\zeta_m = \alpha_0 m / 3 - 2X m^2 / [9(1 + C_{m/3}^{1/2})] - [1 - \log_2(1 + C_{m/3}^{1/2})] / (1 - q) \quad (2)$$

with $C_{\bar{q}} = 1 + 2\bar{q}^2(1-q)X \ln 2$. The formula (2) is independent of n , that is a manifestation of the scale invariance.

² Within the present formulation, the decision cannot be pronounced which of the entropies is underlying the system of turbulence.

³ The scaling relation is a generalization of the one derived first in [28, 29] to the case where the multifractal spectrum has negative values.

The derived scaling exponents (2) are shown in Fig. 1 by the solid curve for the case $\mu = 0.238$, and are compared with experimental data [30] and with the curves given by other theories, i.e., K41 [27], log-normal [21, 22, 23], β -model [31], p-model [32, 26] and log-Poisson [33, 34].

VARIOUS PROBABILITY DENSITY FUNCTIONS

It has been shown that the probability $\Pi_{\phi,S}^{(n)}(x_n)dx_n$ to find a physical quantity x_n in the range $x_n \sim x_n + dx_n$ is given in the form

$$\Pi_{\phi}^{(n)}(x_n)dx_n = \Pi_{\phi,S}^{(n)}(x_n)dx_n + \Delta\Pi_{\phi}^{(n)}(x_n)dx_n \quad (3)$$

with the normalization $\int_{-\infty}^{\infty} dx_n \Pi_{\phi}^{(n)}(x_n) = 1$. The first term represents the contribution by the singular part of the quantity x_n stemmed from the multifractal distribution of its singularities in physical space. This is given by $\Pi_{\phi,S}^{(n)}(|x_n|)dx_n \propto P^{(n)}(\alpha)d\alpha$ with the transformation of the variables, $|x_n| = \delta_n^{\phi\alpha/3}$. Whereas the second term $\Delta\Pi_{\phi}^{(n)}(x_n)dx_n$ represents the contribution from the dissipative term in the Navier-Stokes equation, and/or the one from the errors in measurements. The dissipative term has been discarded in the above investigation for the distribution of singularities since it violates the invariance under the scale transformation. The contribution of the second term provides a correction to the first one. Note that each term in (3) is a multiple of two probability functions, i.e., the one to determine the portion of the contribution among the above mentioned two independent origins, and the other to find x_n in the range $x_n \sim x_n + dx_n$. Note also that the values of x_n originated in the singularity are rather large representing intermittent large deviations, and that those contributing to the correction terms are of the order of or smaller than its standard deviation.

The m th moment of the variable $|x_n|$ is given by $\langle\langle |x_n|^m \rangle\rangle_{\phi} \equiv \int_{-\infty}^{\infty} dx_n |x_n|^m \Pi_{\phi}^{(n)}(x_n) = 2\gamma_{\phi,m}^{(n)} + (1 - 2\gamma_{\phi,0}^{(n)})a_{\phi m} \delta_n^{\zeta_{\phi m}}$ where $2\gamma_{\phi,m}^{(n)} = \int_{-\infty}^{\infty} dx_n |x_n|^m \Delta\Pi_{\phi}^{(n)}(x_n)$, and $a_{3\bar{q}} = \{2/[\sqrt{C_{\bar{q}}}(1 + \sqrt{C_{\bar{q}}})]\}^{1/2}$.

We now derive the PDF, $\hat{\Pi}_{\phi}^{(n)}(\xi_n)$, defined by the relation $\hat{\Pi}_{\phi}^{(n)}(\xi_n)d\xi_n = \Pi_{\phi}^{(n)}(x_n)dx_n$ with the variable $\xi_n = x_n/\langle\langle |x_n|^2 \rangle\rangle_{\phi}^{1/2}$ normalized by the standard deviation $\langle\langle x_n^2 \rangle\rangle_{\phi}^{1/2}$. This PDF is to be compared with the observed PDFs. The variable is related with α by $|\xi_n| = \bar{\xi}_n \delta_n^{\phi\alpha/3 - \zeta_{2\phi}/2}$ with $\bar{\xi}_n = [2\gamma_{\phi,2}^{(n)}\delta_n^{-\zeta_{2\phi}} + (1 - 2\gamma_{\phi,0}^{(n)})a_{2\phi}]^{-1/2}$. It is reasonable to imagine that the origin of intermittent rare events is attributed to the first singular term in (3), and that the contribution from the second term is negligible. We then have for the tail part, i.e., $\xi_n^* \leq |\xi_n| \leq \xi_n^{\max}$,

$$\begin{aligned} \hat{\Pi}_{\phi}^{(n)}(\xi_n)d\xi_n &= \Pi_{\phi,S}^{(n)}(x_n)dx_n \\ &= \bar{\Pi}_{\phi}^{(n)} \frac{\bar{\xi}_n}{|\xi_n|} \left[1 - \frac{1-q}{n} \frac{(3\ln|\xi_n/\xi_{n,0}|)^2}{2\phi^2 X |\ln \delta_n|} \right]^{n/(1-q)} d\xi_n \end{aligned} \quad (4)$$

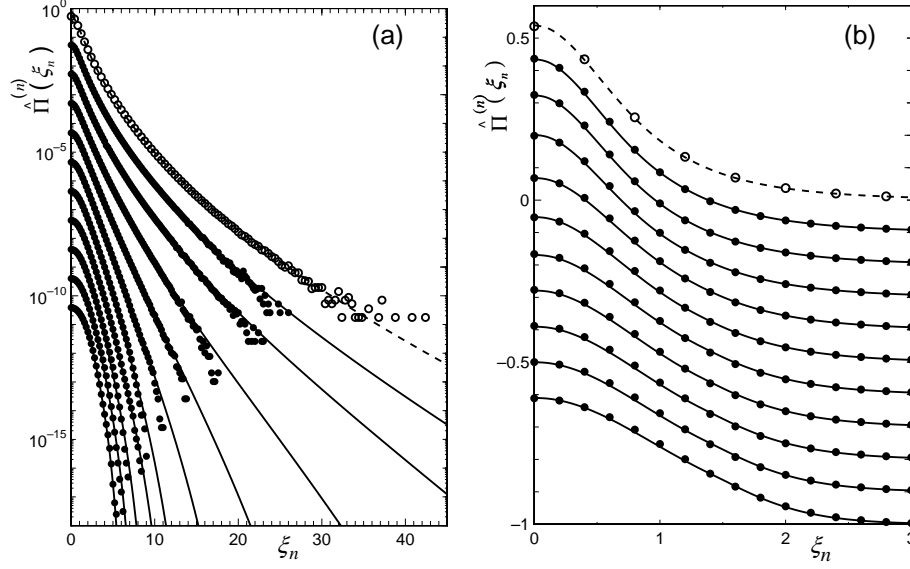


FIGURE 2. Analyses of the PDFs of *velocity fluctuations* (closed circles) and of *velocity derivatives* (open circles) measured in the DNS by Gotoh et al. at $R_\lambda = 380$ by the present theoretical PDFs $\hat{\Pi}^{(n)}(\xi_n)$ for *velocity fluctuations* (solid lines) and for *velocity derivatives* (dashed line) are plotted on (a) log and (b) linear scales. The DNS data points are symmetrized by taking averages of the left and the right hand sides data. The measuring distances, $r/\eta = \ell_n/\eta$, for the PDF of velocity fluctuations are, from the second top to bottom: 2.38, 4.76, 9.52, 19.0, 38.1, 76.2, 152, 305, 609, 1220. For the theoretical PDFs of velocity fluctuations, $\mu = 0.240$ ($q = 0.391$), from the second top to bottom: $(n, \bar{n}, q') = (20.7, 14.6, 1.60)$, $(19.2, 13.1, 1.60)$, $(16.2, 10.1, 1.58)$, $(13.6, 7.54, 1.50)$, $(11.5, 5.44, 1.45)$, $(9.80, 3.74, 1.40)$, $(9.00, 2.94, 1.35)$, $(7.90, 1.84, 1.30)$, $(7.00, 0.94, 1.25)$, $(6.10, 0.04, 1.20)$, $\xi_n^* = 1.10 \sim 1.43$ ($\alpha^* = 1.07$), and $\xi_n^{\max} = 204 \sim 6.63$. For the theoretical PDF of velocity derivatives, $(n, \bar{n}, q') = (22.4, 16.3, 1.55)$, $\xi_n^* = 1.06$ ($\alpha^* = 1.07$), and $\xi_n^{\max} = 302$. For better visibility, each PDF is shifted by -1 unit along the vertical axis.

with $\bar{\Pi}_\phi^{(n)} = 3(1 - 2\gamma_0^{(n)})/(2\phi\bar{\xi}_n\sqrt{2\pi X|\ln\delta_n|})$, $\xi_{n,0} = \bar{\xi}_n\delta_n^{\phi\alpha_0/3 - \zeta_{2\phi}/2}$, $\xi_n^{\max} = \bar{\xi}_n\delta_n^{\phi\alpha_{\min}/3 - \zeta_{2\phi}/2}$. On the other hand, for the center part, the contribution to the PDF comes, mainly, from thermal fluctuations or measurement error. It may be described by the Tsallis distribution function with respect to the variable ξ_n itself, i.e., $|\xi_n| \leq \xi_n^*$,

$$\begin{aligned} \hat{\Pi}_\phi^{(n)}(\xi_n)d\xi_n &= [\hat{\Pi}_{\phi,S}^{(n)}(x_n) + \Delta\hat{\Pi}_\phi^{(n)}(x_n)]dx_n \\ &= \bar{\Pi}_\phi^{(n)} \left\{ 1 - \frac{1-q'}{2} \left(1 + \frac{3f'(\alpha^*)}{\phi} \right) \left[\left(\frac{\xi_n}{\xi_n^*} \right)^2 - 1 \right] \right\}^{1/(1-q')} d\xi_n. \quad (5) \end{aligned}$$

This specific form of the Tsallis distribution function is determined by the condition that the two PDFs (4) and (5) should have the same value and the same slope at ξ_n^* which is defined by $\xi_n^* = \bar{\xi}_n\delta_n^{\phi\alpha^*/3 - \zeta_{2\phi}/2}$ with α^* being the smaller solution of $\zeta_{2\phi}/2 - \phi\alpha/3 + 1 - f(\alpha) = 0$. It is the point at which $\hat{\Pi}_\phi^{(n)}(\xi_n^*)$ has the least n -dependence for large n .

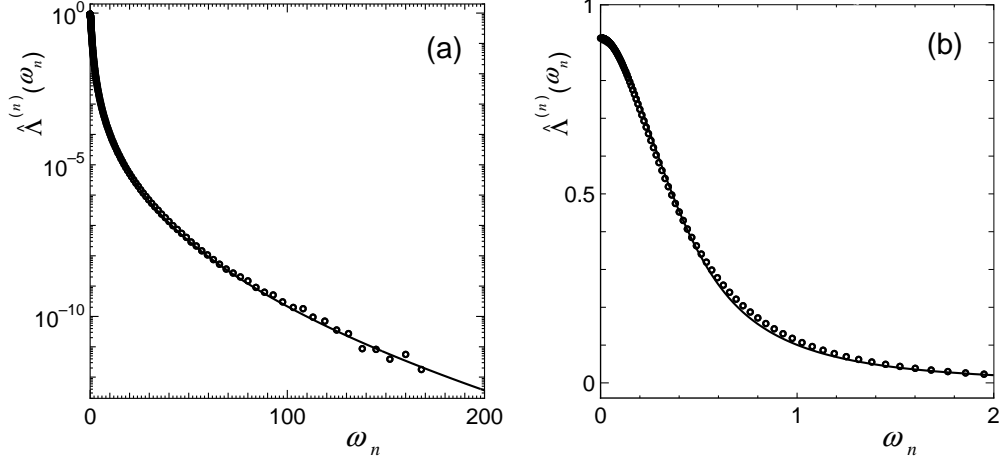


FIGURE 3. Comparison between the PDF of *fluid particle accelerations* measured in the DNS by Gotoh et al. at $R_\lambda = 380$ and the present theoretical PDF $\hat{\Lambda}^{(n)}(\omega_n)$ are plotted on (a) log and (b) linear scales. Closed circles are the DNS data points both on the left and right hand sides of the PDF. Solid lines represent the curves given by the present theory with $\mu = 0.240$ ($q = 0.391$), $(n, \bar{n}, q') = (17.5, 11.4, 1.70)$, $\omega_n^* = 0.622$ ($\alpha^* = 1.01$), and $\omega_n^{\max} = 2530$.

With the help of the second equality in (5), we obtain $\Delta\Pi_\phi^{(n)}(x_n)$, and have the formula to evaluate $\gamma_{\phi,m}^{(n)}$ in the form $2\gamma_{\phi,m}^{(n)} = (K_{\phi,m}^{(n)} - L_{\phi,m}^{(n)}) / (1 + K_{\phi,0}^{(n)} - L_{\phi,0}^{(n)})$ where

$$K_{\phi,m}^{(n)} = \frac{3 \delta_n^{\phi(m+1)\alpha^*/3 - \zeta_{2\phi}/2}}{\phi \sqrt{2\pi X |\ln \delta_n|}} \int_0^1 dz z^m \left[1 - \frac{1-q'}{2} \left(1 + \frac{3f'(\alpha^*)}{\phi} \right) (z^2 - 1) \right]^{1/(1-q')} \quad (6)$$

$$L_{\phi,m}^{(n)} = \frac{3 \delta_n^{\phi m \alpha^*/3}}{\phi \sqrt{2\pi X |\ln \delta_n|}} \int_{z_{\min}^*}^1 dz z^{m-1} \left[1 - \frac{1-q}{n} \frac{(3 \ln |z/z_0^*|)^2}{2\phi^2 X |\ln \delta_n|} \right]^{n/(1-q)} \quad (7)$$

with $z_{\min}^* = \xi_{\min}/\xi_n^* = \delta_n^{\phi(\alpha_{\max} - \alpha^*)/3}$, $z_0^* = \xi_{n,0}/\xi_n^* = \delta_n^{\phi(\alpha_0 - \alpha^*)/3}$. We see that the tail part of the PDF, given by (4), is mostly determined by the intermittency exponent μ and the multifractal depth n which gives a length scale ℓ_n . On the other hand, the center part of the PDF, (5), is mainly controlled by q' .

The PDFs both for velocity fluctuations and for velocity derivatives are given by the common formula $\hat{\Pi}^{(n)}(\xi_n) \equiv \hat{\Pi}_{\phi=1}^{(n)}(\xi_n)$ in their normalized variables $\xi_n = \delta u_n / \langle \langle (\delta u_n)^2 \rangle \rangle^{1/2}$. On the other hand, the PDFs both for pressure differences and for fluid particle accelerations are given by the common formula $\hat{\Lambda}^{(n)}(\omega_n) \equiv \hat{\Pi}_{\phi=2}^{(n)}(\omega_n)$ in their normalized variables $\omega_n = \delta p_n / \langle \langle (\delta p_n)^2 \rangle \rangle^{1/2}$. The PDF for energy dissipation rates is given with $\phi = 3$.

The PDFs extracted by Gotoh et al. from their DNS data [13] at $R_\lambda = 380$ are shown, on log and linear scales, in Fig. 2 both for *velocity fluctuations* and for *velocity derivatives*, and in Fig. 3 for *fluid particle accelerations*. We found the value $\mu = 0.240$ by analyzing the measured scaling exponents ζ_m of velocity structure function with the

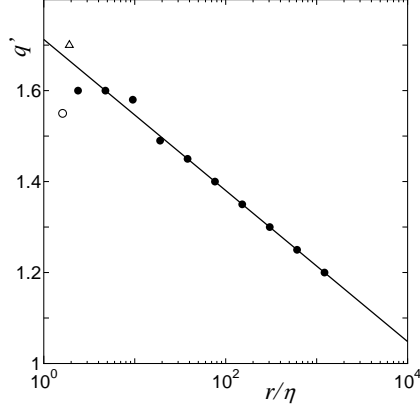


FIGURE 4. Dependence of q' on the distance r/η extracted from the analyses of the PDFs for velocity fluctuations (closed circles), for velocity derivatives (open circle) and for fluid particle accelerations (open triangle). The line represents $q' = -0.05 \log_2(r/\eta) + 1.71$.

formula (2), which gives the values $q = 0.391$, $\alpha_0 = 1.14$ and $X = 0.285$. Through the analyses of the PDFs for velocity fluctuations in Fig. 2, we extracted the formula for the dependence of n on r/η : [7, 8]

$$n = -0.989 \times \log_2 r/\eta + 16.1 \quad (\text{for } \ell_c \leq r), \quad (8)$$

$$n = -2.40 \times \log_2 r/\eta + 24.0 \quad (\text{for } r < \ell_c). \quad (9)$$

This shows that the inertial range is divided into two scaling regions separated by the characteristic length $\ell_c/\eta = 48.7$ which is close to the Taylor microscale $\lambda/\eta = 38.3$ of the system. The equation (8) is consistent with the picture of the energy cascade model in which each eddy breaks up into 2 pieces at every cascade steps, whereas (9) indicates that, for $r < \ell_c$, each eddy breaks up, effectively, into $1.33 \approx 4/3$ [8] pieces at every cascade steps. This fact may be attributed to a manifestation of structural difference of eddies, which can be checked by visualizing DNS eddies. Actually, one observes that DNS eddies with larger diameters than Taylor microscale λ have rather round shapes, whereas eddies with smaller diameters compared with λ have rather stretched shapes [35]. The energy input scale for this DNS is estimated as the longest scale available in the lattice with cyclic boundary condition, i.e., $\ell_{\text{in}}/\eta = \pi/\eta \approx 1220$ with $\eta \approx 0.258 \times 10^{-2}$ [13] which gives the number of steps \bar{n} within the energy cascade model through the formula (1) with $\ell_0/\eta \approx 81300$ determined by (8).

For the analysis of the PDF for velocity derivatives in Fig. 2, we chose the value $(n, \bar{n}, q') = (22.4, 16.3, 1.55)$. The length corresponding to n is calculated by (9) to give $r/\eta = 1.61$, which may provide us with an estimate for the effective shortest length in processing the DNS data to extract velocity derivatives. Note that it is about the same order of the mesh size $\Delta r/\eta = 2\pi/(1024 \times \eta) \approx 2.38$ [13] of the DNS lattice.

For the PDFs for *fluid particle accelerations* in Fig. 3, we have $(n, \bar{n}, q') = (17.5, 11.4, 1.70)$. Substitution of this value into (9) gives the corresponding characteristic length $r/\eta = 7.91$ [11]. This may be the effective minimum resolution in cooking the DNS data to distill accelerations.

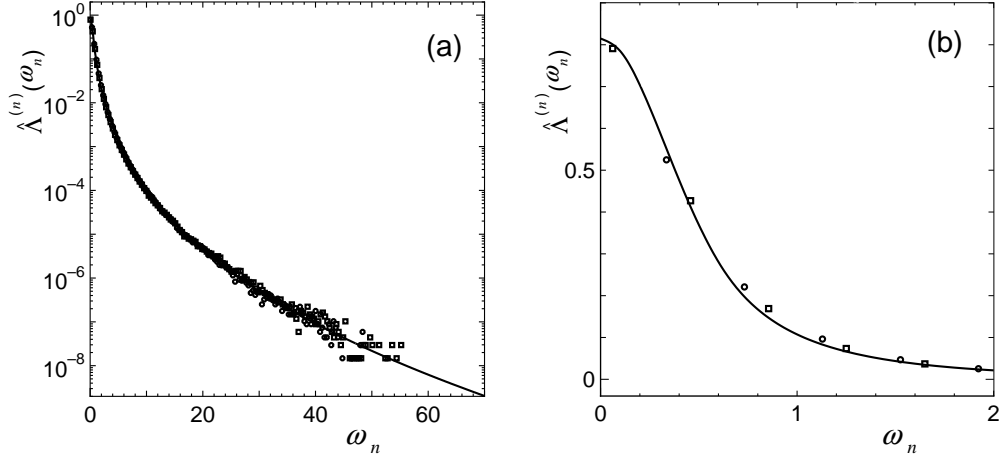


FIGURE 5. Comparison between the experimentally measured PDF of *fluid particle accelerations* by Bodenschatz et al. at $R_\lambda = 690$ ($Re = 31\,400$) and the present theoretical PDF $\hat{\Lambda}^{(n)}(\omega_n)$ are plotted on (a) log and (b) linear scales. Open squares are the experimental data points on the left hand side of the PDF, whereas open circles are those on the right hand side. Solid lines represent the curves given by the present theory with $\mu = 0.240$ ($q = 0.391$), $(n, q') = (17.1, 1.45)$, $\omega_n^* = 0.605$ ($\alpha^* = 1.01$), and $\omega_n^{\max} = 2040$.

In Fig. 4, we plotted the dependence of q' on the distance r/η extracted from the analyses of the DNS data, i.e., the closed circles are extracted from the PDF of velocity fluctuations, the open circle is from the PDF of velocity derivatives and the open triangle from the PDF of fluid particle accelerations. The line represents $q' = -0.05 \log_2(r/\eta) + 1.71$. The points for $r/\eta > 20$ (closed circles) and for the accelerations (open triangle) are quite sensitive and easy to be determined. Other points are insensitive and have a rather wide range in deciding the values q' .

The PDFs for fluid particle accelerations measured by Bodenschatz et al. at $R_\lambda = 690$ [16] are given in Fig. 5. We determined the value $n = 17.1$ by substituting the reported value $\ell_0 = \ell_{\text{in}} = 7.1$ cm and the spatial resolution $0.5 \mu\text{m}$ of the measurement for ℓ_n into its definition, $n = \log_2(\ell_0/\ell_n)$. The values $\mu = 0.240$ and $q' = 1.45$ are extracted by the analysis of the experimental PDF with the derived theoretical formula [11]. Then, we have the values of parameters: $q = 0.391$, $\alpha_0 = 1.14$ and $X = 0.285$. The flatness of the PDF turns out to be [11] $F_a^{(n)} \equiv \langle\langle a_n^4 \rangle\rangle / \langle\langle a_n^2 \rangle\rangle^2 = \langle\langle \xi_n^4 \rangle\rangle = 56.9$ which is compatible with the value of the flatness $\sim 55 \pm 4$ reported in [16].

DISCUSSIONS AND PROSPECTS

In this paper, the various experimental PDFs in turbulence are analyzed precisely with the formulae (4) and (5) of the corresponding PDFs derived by the MFA. It is revealed that there are two distinct mechanisms underlying the dynamics of turbulence. One contributes to the *tail* part of PDFs and the other to the *center* part. The structure of the tail part of the PDFs is determined by the global structure representing the intermittent large deviations that is manifestations of the multifractal distribution of singularities

in physical space due to the scale invariance of the Navier-Stokes equation for large Reynolds number. The specific form of the tail part comes from the assumption that the probability to find a singularity exponent α within the range $\alpha \sim \alpha + d\alpha$ at a point in physical space is given by the Tsallis-type distribution function with the Tsallis parameter q . The relation between α and an observing variable is given by the scale transformation. On the other hand, the structure of the center part represents small deviations violating the scale invariance due to thermal fluctuations and/or observation error. The center part is assumed to be given by the Tsallis-type distribution function with the Tsallis parameter q' for the observing variable itself. The value of q' may be determined by a local structure of the system, e.g., the dynamics of a vortex, the mutual interaction between vortices and so on, and depends on the distance of two measuring points in contrast to q . The latter parameter q does not depend on the distance, and is determined once the value of the intermittency exponent is given. It is one of the attractive future problems to derive two different dynamics taking care of the tail part controlled by q and the center part by q' , and will be reported in the near future.

The success of the MFA in analyzing turbulence in high accuracy may provide us with a good tool to see what is the origin of the singularities and why their distribution is multifractal. In order to investigate them, the vortex tangle is one of the attractive candidates as Feynman proposed [36], since the vorticity in superfluid ^4He and ^3He is quantized and the normal component within the sense of the two fluid model can be negligible at very low temperature. If the singularity originates from the core of vortex, the multifractality of turbulence in normal fluid can be related to various values of vorticities in the fluid. In this case, the vortex tangle may be uni-fractal, and does not exhibit intermittency. If the singularity originates from the reconnection of vortices, the multifractality of turbulence in normal fluid is related to the distribution of reconnection points in the fluid. Then, the vortex tangle may be also multifractal, and does exhibit intermittency. A temperature-independent vortex decay mechanism below $T \sim 70$ mK has been observed in superfluid ^4He [37], and the Kolmogorov spectrum (K41) is extracted from the simulation within the vortex filament model for non-frictional superfluid ^4He [38]. In tangle, the quantized vortex crosses the stream lines of superfluid velocity field, which may result in the decay mechanism at low temperature. We expect that, through the analysis of the local dynamics controlled by the Tsallis parameter q' , we can extract some information about the mutual friction between the superfluid and normal components.

A circular vortex lattice is observed in the simulation of fast rotating Bose-Einstein condensate confined in a 2-dimensional quadratic-plus-quartic potential [39]. A possibility of generation of tangle phase in this system is one of the attractive problems. The situation may be quite similar to the one in the generation of the Taylor-Couette turbulence in normal fluid.

Let us close this paper by mentioning that the vortex tangle can be an important stationary phase of *quLSI* (quantum LSI) consisting of, for example, a huge number of superconducting loops of flux qubit [40]. The direction of current in a loop may change so quickly under an operation of quantum computer. The congeries of the flux qubits can produce a tangle phase of flux quantum. It may be important to see if the tangle phase benefits quantum entangled states or not.

ACKNOWLEDGMENTS

The authors would like to thank Prof. R.H. Kraichnan and Prof. C. Tsallis for their fruitful and enlightening comments with encouragement, and are grateful to Prof. E. Bodenschatz and Prof. T. Gotoh for the kindness to show their data prior to publication.

REFERENCES

1. T. Arimitsu and N. Arimitsu, *Phys. Rev. E* **61**, 3237-3240 (2000).
2. T. Arimitsu and N. Arimitsu, *J. Phys. A: Math. Gen.* **33**, L235-L241 (2000) [CORRIGENDUM: **34**, 673-674 (2001)].
3. T. Arimitsu and N. Arimitsu, *Chaos, Solitons and Fractals* **13**, 479-489 (2002).
4. T. Arimitsu and N. Arimitsu, *Prog. Theor. Phys.* **105**, 355-360 (2001).
5. T. Arimitsu and N. Arimitsu, *Physica A* **295**, 177-194 (2001).
6. N. Arimitsu and T. Arimitsu, *J. Korean Phys. Soc.* **40**, 1032-1036 (2002).
7. T. Arimitsu and N. Arimitsu, *Physica A* **305**, 218-226 (2002).
8. T. Arimitsu and N. Arimitsu, *J. Phys.: Condens. Matter* **14**, 2237-2246 (2002).
9. N. Arimitsu and T. Arimitsu, *Europhys. Lett.* **60**, 60-65 (2002).
10. T. Arimitsu and N. Arimitsu, *Condensed Matter Physics* **6** 85-92 (2003).
11. T. Arimitsu and N. Arimitsu, cond-mat/0210274 (2002).
12. T. Arimitsu and N. Arimitsu, cond-mat/0301516 (2003).
13. T. Gotoh, D. Fukayama and T. Nakano, *Phys. Fluids* **14**, 1065-1081 (2002).
14. A. La Porta, et al., *Nature* **409**, 1017-1019 (2001).
15. G. A. Voth, et al., *J. Fluid Mech.* **469**, 121-160 (2002).
16. A. M. Crawford, N. Mordant and E. Bodenschatz, (2002) physics/0212080.
17. C. Tsallis, *J. Stat. Phys.* **52**, 479-487 (1988).
18. C. Tsallis, *Braz. J. Phys.* **29**, 1-35 (1999); See recent progresses at <http://tsallis.cat.cbpf.br/biblio.htm>.
19. A. Rényi, "On measures of entropy and information" in *Proc. 4th Berkeley Symp. Maths. Stat. Prob.* **1**, 547 (1961).
20. J.H. Havrda and F. Charvat, *Kybernetika* **3**, 30-35 (1967).
21. A.M. Oboukhov, *J. Fluid Mech.* **13**, 77-81 (1962).
22. A.N. Kolmogorov, *J. Fluid Mech.* **13**, 82-85 (1962).
23. A.M. Yaglom, *Sov. Phys. Dokl.* **11**, 26-29 (1966).
24. S. S. Moiseev, A. V. Tur and V. V. Yanovskii, *Sov. Phys. JETP* **44**, 556-561 (1976).
25. U. Frisch and G. Parisi, "On the singularity structure of fully developed turbulence" in *Turbulence and Predictability in Geophysical Fluid Dynamics and Climate Dynamics*, ed. by M. Ghil, R. Benzi and G. Parisi, North-Holland, New York, 1985, p84.
26. C. Meneveau and K. R. Sreenivasan, *Nucl. Phys. B (Proc. Suppl.)* **2**, 49-76 (1987).
27. A.N. Kolmogorov, *Dokl. Akad. Nauk SSSR* **30**, 301-305 (1941); *ibid.* **31**, 538-540 (1941).
28. U.M.S. Costa, M.L. Lyra, A.R. Plastino and C. Tsallis, *Phys. Rev. E* **56**, 245-250 (1997).
29. M.L. Lyra and C. Tsallis, *Phys. Rev. Lett.* **80**, 53-56 (1998).
30. C. Meneveau and K. R. Sreenivasan, *J. Fluid Mech.* **224**, 429-484 (1991).
31. U. Frisch, P-L. Sulem and M. Nelkin, *J. Fluid Mech.* **87**, 719-736 (1978).
32. C. Meneveau and K. R. Sreenivasan, *Phys. Rev. Lett.* **59**, 1424-1427 (1987).
33. Z-S. She and E. Leveque, *Phys. Rev. Lett.* **72**, 336-339 (1994).
34. Z-S. She and E. Waymire, *Phys. Rev. Lett.* **74**, 262-265 (1995).
35. Private communication with Prof. M. Tanahashi at Tokyo Institute of Technology.
36. R. P. Feynman, "Application of quantum mechanics to liquid helium" in *Progress in Low Temperature Physics*, ed. by C. J. Gorter, North Holland, Amsterdam, 1955, p17.
37. S.I. Davis, P.C. Hendry and P.V.E. McClintock, *Physica B* **280**, 43-44 (2000).
38. T. Araki, M. Tsubota and S.K. Nemirovskii, *Phys. Rev. Lett.* **89**, 145301 (2002).
39. K. Kasamatsu, M. Tsubota and M. Ueda, *Phys. Rev. A* **66**, 053606 (2002).
40. I. Chiorescu et al., *Science* **299**, 1869-1871 (2003).